

Scattering in the Attractive Yukawa Potential in the Limit of Strong Interaction

S. A. Khrapak,* A. V. Ivlev, and G. E. Morfill

Centre for Interdisciplinary Plasma Science, Max-Planck-Institut für Extraterrestrische Physik, D-85740 Garching, Germany

S. K. Zhdanov

Moscow Engineering Physics Institute, Kashirskoe shosse, 31, 115409, Moscow, Russia

(Received 29 October 2002; published 6 June 2003)

Scattering in the attractive screened Coulomb (Yukawa) potential in the limit of strong interaction is investigated. It is shown that the scattering occurs mostly with large angles. The corresponding momentum-transfer cross section is calculated. The results are applied to estimate the ion drag force acting on an isolated micron-sized grain in low-pressure bulk plasmas.

DOI: 10.1103/PhysRevLett.90.225002

PACS numbers: 52.27.Lw, 52.20.Hv

The screened Coulomb (Debye-Hückel or Yukawa) potential is widely used in physics, being a good approximation to describe interaction between charged particles in (dusty/complex) plasmas, colloidal suspensions, etc. In this Letter we report an analytical approach (based on our numerical calculations) to obtain the momentum-transfer cross section for pair collisions of particles interacting via the attractive Yukawa potential. We consider the limit when interaction is so strong that the scattering is mostly with large angles. This limit is opposite to the well-known theory of Coulomb scattering and is of interest when (at least) one of the particles is highly charged and/or their relative velocity is small. As an example we apply the obtained results to estimate the ion drag force acting on a negatively charged micrograin in a bulk plasma.

Let us consider collision between two particles of masses m_1 and m_2 interacting via isotropic potential $U(r)$. This problem is equivalent to the scattering of a single particle of reduced mass, $m = m_1 m_2 / (m_1 + m_2)$, in a field $U(r)$ (whose center is at the center of masses). First, we study the case of pointlike particles; the role of finite sizes is addressed later. Introducing the relative velocity, v , and the impact parameter, ρ , we get the deflection angle, $\chi(\rho) = |\pi - 2\varphi(\rho)|$, where [1]

$$\varphi(\rho) = \rho \int_{r_0}^{\infty} \frac{dr}{r^2 \sqrt{1 - U_{\text{eff}}(r, \rho)}}. \quad (1)$$

Here U_{eff} is the effective potential energy (normalized by the kinetic energy, $\frac{1}{2}mv^2$),

$$U_{\text{eff}}(r, \rho) = \rho^2/r^2 + 2U(r)/mv^2. \quad (2)$$

The scattering momentum-transfer cross section is given by

$$\sigma_s = 2\pi \int_0^{\infty} [1 - \cos\chi(\rho)]\rho d\rho. \quad (3)$$

Integration in (1) is performed from the distance of the closest approach, $r_0(\rho)$ — the largest root of the equation

$$U_{\text{eff}}(r, \rho) = 1. \quad (4)$$

Using Eqs. (1)–(4), the momentum-transfer cross section σ_s can be in general calculated for arbitrary potential $U(r)$.

For the Yukawa potential, $U(r) = -(U_0/r)e^{-r/\lambda}$ (where λ is the screening length and U_0 is positive for attraction), the following important parameter can be introduced:

$$\beta(v) = U_0/mv^2\lambda, \quad (5)$$

which is the ratio of the Coulomb radius, $r_C = U_0/mv^2$, to the screening length λ . Normalizing r and ρ by the screening length, we get that β is the only parameter the function $U_{\text{eff}}(r, \rho)$ depends on. The same applies for the deflection angle $\chi(\rho)$ [see Eq. (1)]. Therefore, we conclude from Eq. (3) that σ_s/λ^2 depends only on β and, hence, Eq. (5) defines a *unique parameter* which describes scattering for Yukawa interaction.

The standard Coulomb scattering approach (Coulomb potential with cutoff at $\rho = \lambda$) which is widely used to describe collisions in usual electron-ion plasma deals with the situation $\beta \ll 1$. For example, for electron-ion collisions in an isotropic plasma $\beta(v_{T_e}) = e^2/T_e\lambda \sim N_D^{-1} \ll 1$ (where $v_{T_e} = \sqrt{T_e/m_e}$ is the thermal velocity of electrons, λ is plasma Debye length, and N_D is a number of electrons inside the Debye sphere). In this case the interaction can be called “weak,” in the sense that its range—the Coulomb radius $r_C = e^2/T_e$ —is much smaller than the screening length λ . The ratio of the momentum transfer by the electrons with $r_C < \rho < \lambda$ to that with $\rho < r_C$ is approximately equal to the so-called Coulomb logarithm, $\Lambda = \ln(1/\beta) \gg 1$. The relative contribution of electrons with $\rho > \lambda$ is small, $\sim \Lambda^{-1}$, because of the screening [2]. Therefore, the momentum transfer is mostly associated with the scattering in the bare Coulomb potential. This justifies the standard Coulomb scattering approach in the limit $\beta \ll 1$. Most of the contribution to the momentum transfer in this case is due to small angle scattering (the electrons are deflected strongly only if $\rho \lesssim r_C$).

The standard Coulomb scattering approach fails when $\beta \gtrsim 1$. In this case the interaction range exceeds the

screening length and deflection can be strong even if $\rho > \lambda$. It was shown recently [3] that the extension of the standard Coulomb scattering theory is possible by taking into account collisions with impact parameters above λ . This basically leads to modification of the Coulomb logarithm. Although the approach of [3] is not rigorous, it shows very good agreement with the earlier numerical results of Refs. [4,5] up to $\beta \approx 5$.

In this Letter we study the case $\beta \gg 1$ (strong interaction). This limit is opposite to the standard Coulomb scattering theory and requires a new physical approach which is formulated below. We start with a brief description of radial motion of particles interacting via the attractive Yukawa potential in terms of the effective potential energy [5,6]. For nonzero impact parameters $U_{\text{eff}}(r, \rho)$ has the following asymptotes: $\lim_{r \rightarrow 0} U_{\text{eff}} = \infty$ and $\lim_{r \rightarrow \infty} U_{\text{eff}} = 0$. Therefore, Eq. (4), which determines the distance of the closest approach, $r_0(\rho)$, always has at least one solution. However, the analysis shows that U_{eff} does not decrease monotonically with r but can deliver local maximum and minimum, so that Eq. (4) can have multiple roots (two or three) for certain conditions. Physically, this means that the potential barrier emerges and then the largest root of Eq. (4) must be chosen for $r_0(\rho)$. For $\beta < \beta_{\text{cr}} \approx 13.2$ there is no barrier for any ρ [5] and the particles can approach close to each other (single root, $r_0 < \lambda$, “close collisions”). For $\beta > \beta_{\text{cr}}$ there exists a critical (transitional) impact parameter, $\rho_*(\beta)$, separating trajectories in two groups: no barrier for $\rho < \rho_*$, but for $\rho > \rho_*$ the barrier emerges and the particles are reflected at much farther distances (three roots, r_0 , significantly exceed λ , “far collisions”). This causes a discontinuity at the curve $r_0(\rho)$ at $\rho = \rho_*$ [3] (two roots, “transition collision”). This also implies a singularity at $\rho = \rho_*$ for the dependence of the scatter-

ing angle χ on ρ : In the vicinity of maximum of U_{eff} we have an expansion: $(1 - U_{\text{eff}})|_{\rho \rightarrow \rho_*} \propto (r - r_{\text{max}})^2 + O(r - r_{\text{max}})^3$, where r_{max} is the location of the maximum. In accordance with Eq. (1) this causes a logarithmic divergency of the scattering angle at $\rho = \rho_*$, which is illustrated in Figs. 1 and 2. Thus, the existence of the potential barrier at $\beta > \beta_{\text{cr}}$ and the discontinuities it induces play a crucial role for the analysis of collisions.

The appearance of the potential barrier and the location of its maximum (i.e., ρ_* and r_{max}) are determined by three conditions [5]: (i) $U_{\text{eff}}(r_{\text{max}}, \rho_*) = 1$; (ii) $U'_{\text{eff}}(r_{\text{max}}, \rho_*) = 0$; (iii) $U''_{\text{eff}}(r_{\text{max}}, \rho_*) < 0$, where primes denote derivatives with respect to r . All three conditions can be satisfied simultaneously only for $\beta \geq \beta_{\text{cr}} \approx 13.2$. The maximum, $r_{\text{max}}(\beta)$, is the solution of the transcendent equation $(r_{\text{max}}/\lambda)e^{r_{\text{max}}/\lambda} = \beta(r_{\text{max}}/\lambda - 1)$. It grows with β monotonically, starting from $r_{\text{max}}(\beta_{\text{cr}})/\lambda = (1 + \sqrt{5})/2 \approx 1.62$. Conditions (i) and (ii) determine the transitional impact parameter, ρ_* , as a function of r_{max} (and thus of β),

$$\rho_* = r_{\text{max}} \sqrt{\frac{r_{\text{max}}/\lambda + 1}{r_{\text{max}}/\lambda - 1}}, \quad (6)$$

which also increases, starting from $\rho_*(\beta_{\text{cr}})/\lambda \approx 3.33$. For large β we obtain the asymptotic solutions: $r_{\text{max}}/\lambda \approx \ln \beta - \ln^{-1} \beta$ and $\rho_*/\lambda \approx \ln \beta + 1 - \frac{1}{2} \ln^{-1} \beta$.

We integrated Eqs. (1) and (3) numerically and obtained the scattering angle and momentum-transfer cross section for various $\beta > \beta_{\text{cr}}$. The dependence of the scattering angle on the impact parameter shown in Fig. 2 has the following features: For close collisions we have $\chi \rightarrow \pi$ at $\rho \rightarrow 0$, and $\chi(\rho)$ grows monotonically until $\rho = \rho_*$, where it diverges; for far collisions the scattering angle decreases very fast, due to exponential screening of

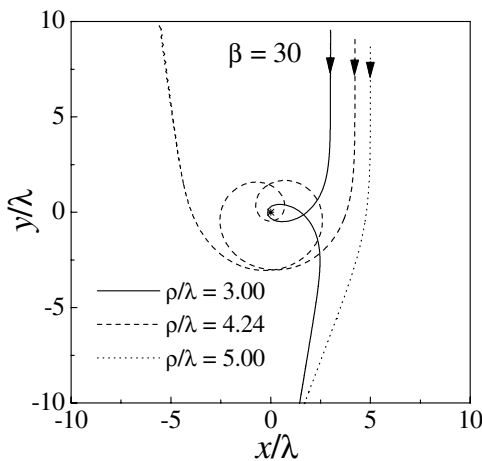


FIG. 1. Particle trajectories during collisions for different impact parameters, ρ . Interaction is via the attractive Yukawa potential. A *unique* parameter characterizing the scattering, β , is equal to 30. Impact parameters are chosen to be below, about, and above the transitional impact parameter, $\rho_* \approx 4.24\lambda$.

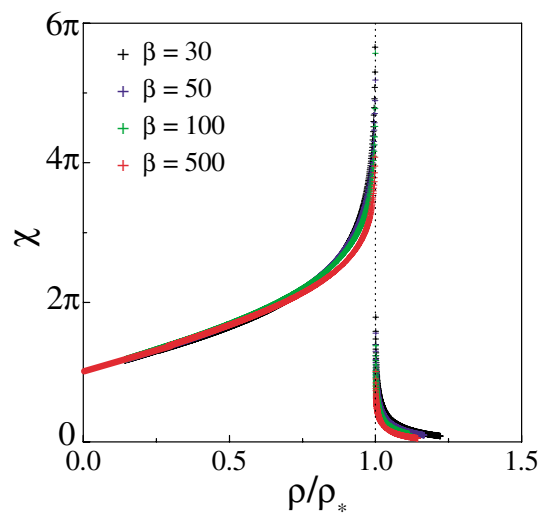


FIG. 2 (color). Scattering angle χ versus the normalized impact parameter ρ/ρ_* (ρ_* is the transitional impact parameter). The numerical calculations are for four different scattering parameters β .

the interaction potential. It is convenient to consider the contribution of close and far collisions to the momentum-transfer cross section separately.

Close collisions ($\rho < \rho_*$).—As can be seen from Fig. 2, the behavior of χ as a function of the normalized impact parameter ρ/ρ_* is *practically independent* of β for $\rho < \rho_*$. This self-similarity, which is one of our most important findings, allows us to present this contribution to the cross section in the form $\sigma_s^{\text{close}} \simeq \mathcal{A} \pi \rho_*^2$, where $\mathcal{A} = 2 \int_0^1 [1 - \cos \chi(\xi)] \xi d\xi$ and $\xi = \rho/\rho_*$. The coefficient \mathcal{A} can be determined by direct numerical integration. We found that $\mathcal{A} = 0.81 \pm 0.01$ for all β in the range $\beta_{\text{cr}} \leq \beta \leq 500$.

Far collisions ($\rho > \rho_*$).—Contribution of far collisions to the cross section can be estimated in the following way. The scattering angle decays rapidly in the vicinity of ρ_* , as $\chi \sim (1/2\sqrt{\rho_*}) \ln[1/(\rho - \rho_*)]$, so that the range $\rho - \rho_*$ for the large angle scattering is $\propto e^{-2\sqrt{\rho_*}}$. Therefore, the contribution of the large angle scattering, $\propto \rho_* e^{-2\sqrt{\rho_*}}$, vanishes rapidly as β grows (see also Fig. 2). Then the small angle approximation is applicable, yielding $\sigma_s^{\text{far}}(\beta)/\lambda^2 = \text{const} + O(\ln^{-1}\beta)$. This functional dependence is in agreement with numerically found $\sigma_s^{\text{far}}(\beta)/\lambda^2 \simeq 6.4(1 + 2.0\ln^{-1}\beta)$. Note that the ratio $\sigma_s^{\text{far}}/\sigma_s^{\text{close}}$ decreases with β : It is ~ 0.3 for $\beta = \beta_{\text{cr}}$ and tends to zero as $\propto \ln^{-2}\beta$.

Combining the contribution from close and far collisions, we can write the momentum-transfer cross section in the form

$$\sigma_s(\beta) \simeq \mathcal{A} \pi \rho_*^2(\beta) + \mathcal{B} \lambda^2 (1 + 2.0 \ln^{-1} \beta), \quad (7)$$

where $\mathcal{A} \simeq 0.81$, $\mathcal{B} \simeq 6.4$, and $\rho_* \simeq \lambda(\ln \beta + 1 - \frac{1}{2} \ln^{-1} \beta)$. This expression is valid for $\beta \geq \beta_{\text{cr}}$ and pointlike particles. Figure 3 demonstrates very good agreement between Eq. (7) and numerical calculations. Here we also show an analytical approximation obtained earlier by Khrapak *et al.* valid for $\beta \lesssim 5$ [3]. Note that the standard Coulomb scattering theory yielding $\sigma_s = 2\pi\lambda^2\beta^2 \ln(1 + 1/\beta^2)$, underestimates the cross section significantly for $\beta \gtrsim 1$.

Now let us study the collision of two (spherical) particles interacting via the attractive Yukawa potential and having *finite radii* (a_1 and a_2). This problem is equivalent to the scattering of a pointlike particle at the center of radius $a = a_1 + a_2$. In contrast to the case of pointlike particles, when the scattering is described by the single parameter β , now we have a second parameter, a/λ . This implies the following difference: If the distance of the closest approach, r_0 [calculated from Eq. (4)], is smaller than a , then the direct collision takes place. In this case we assume an agglomeration; i.e., the pointlike particle is collected (absorbed) by the center. Collection occurs if the particle has an impact parameter smaller than the so-called “collection radius,” ρ_c . If $\rho_c < \rho_*$, then Eq. (4) has a single root and the orbital motion limited (OML) theory can be applied yielding

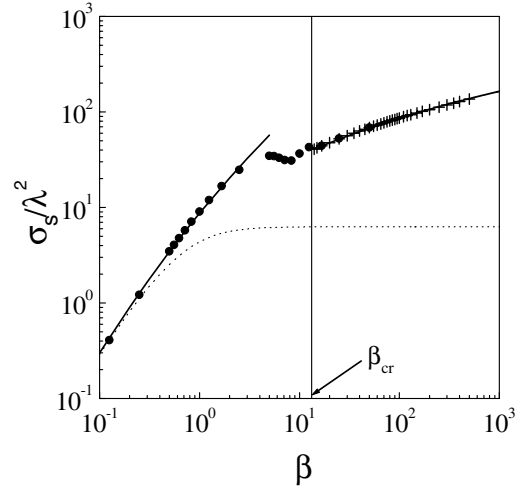


FIG. 3. Momentum-transfer cross section, σ_s , normalized to the squared screening length, λ^2 , versus the scattering parameter, β . Our numerical calculation (+) and earlier numerical results by Hahn *et al.* [4] (●) are shown. The analytical expression [Eq. (7), solid line] fits quite well the numerical calculations for $\beta > \beta_{\text{cr}}$. The analytical formula proposed in Ref. [3] agrees well with the numerical results for $\beta \lesssim 5$. The dotted line represents the standard Coulomb scattering theory.

$$\begin{aligned} \rho_c &= a\sqrt{1 + 2U(a)/mv^2} \equiv a\sqrt{1 + 2\beta(\lambda/a)e^{-a/\lambda}} \\ &\equiv \rho_c^{\text{OML}}. \end{aligned} \quad (8)$$

At very large β , however, ρ_c^{OML} exceeds the transitional impact parameter, $\rho_* \simeq \lambda \ln \beta$. That means that the OML approach is no longer applicable because for particles having $\rho \geq \rho_*$ Eq. (4) has multiple roots. These particles experience far collisions, with r_0 considerably larger than λ and therefore are not absorbed (we assume $a \lesssim \lambda$). Thus the absorption radius for very large β equals the transitional impact parameter: $\rho_c = \rho_*$.

The total momentum-transfer cross section for the case of finite size particles consists of collection and scattering parts: $\sigma_\Sigma = \sigma_c + \tilde{\sigma}_s$. Collection formally corresponds to the scattering angle $\chi = \pi/2$, yielding $\sigma_c = \pi\rho_c^2$. The scattering part $\tilde{\sigma}_s$ is given now by Eq. (3), with the lower limit of integration replaced by ρ_c . The dependence $\sigma_\Sigma(\beta)$ is shown in Fig. 4 for different values of a/λ . For pointlike particles ($a/\lambda = 0$, solid line) the total cross section is determined by Eq. (7). Collection is not important when $2\beta(a/\lambda) \ll \ln^2\beta$ (i.e., $\rho_c \ll \rho_*$). Therefore, for finite but relatively small particles ($a/\lambda \lesssim 10^{-2}$) we have $\sigma_\Sigma \simeq \sigma_s$ in the considered range of β ; i.e., the momentum transfer is mostly associated with the elastic scattering. For larger particles collection becomes more important: One can see from Fig. 4 that the momentum transfer can decrease or increase (in comparison with the case of a pointlike particle), depending on the value of β . For sufficiently large β (when $\rho_c = \rho_*$) the total cross section is $\sigma_\Sigma = \pi\rho_*^2 + \sigma_s^{\text{far}}$ (dotted line). At $\beta \rightarrow \infty$ the contribution of elastic (far) collisions

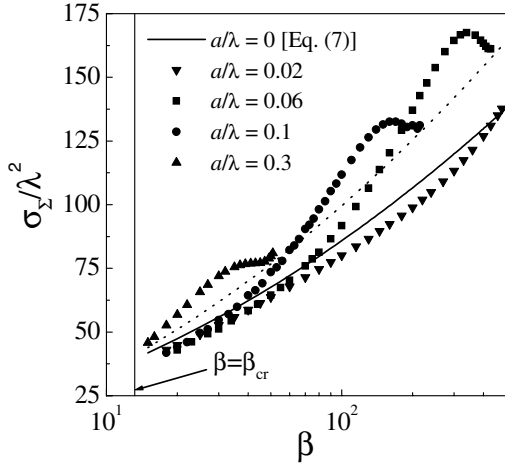


FIG. 4. The total momentum-transfer cross section, σ_{Σ} , normalized to the squared screening length, λ^2 , versus the scattering parameter, β . The numerical results for different values of a/λ are shown to illustrate the role of the finite particle radius, a . The dotted line corresponds to $\sigma_{\Sigma} = \pi\rho_*^2 + \sigma_s^{\text{far}}$.

vanishes (the momentum transfer is entirely associated with the collection) and σ_{Σ} tends to $\pi\rho_*^2$; i.e., σ_{Σ} is asymptotically $\mathcal{A}^{-1} \approx 1.23$ times larger than σ_s . Hence, the momentum transfer is not very sensitive to the particle size—the deviation of σ_{Σ} from σ_s does not exceed $\sim 50\%$. This allows us to draw a very important conclusion that for practical purposes the total momentum-transfer cross section can be quite well approximated by $\sigma_{\Sigma} \sim \pi\rho_*^2$.

Finally, we apply the obtained results to estimate the ion drag force acting on an isolated μm -size grain in a bulk low-pressure plasma. This force is associated with the momentum transfer due to the relative ion drift and determines various important processes in complex (dusty) plasmas [3,7–12]. We restrict ourselves to the situation of subthermal relative drift, $u \ll v_{T_i}$, which corresponds to a slow grain motion and/or the ion drift in a weak electric field. Even a weak plasma anisotropy induced by the drift can cause the deviation of the grain potential from the Yukawa form: The potential does not fall off exponentially at very large distances, $r \gg \lambda$, but exhibits $\propto r^{-3}$ asymptotic behavior [13,14]. In addition, the plasma absorption on a grain can cause a $\propto r^{-2}$ asymptote at large r [7]. However, in Ref. [5] it was shown that this deviation does not affect substantially the momentum-transfer cross section. Therefore, for our problem the attractive Yukawa interaction potential between positive ions and a negatively charged grain is a good approximation. The interaction is characterized by $U_0 = e|\phi_s|ae^{a/\lambda}$ (where $\phi_s < 0$ is the grain surface potential). The plasma screening is mostly associated with ions, $\lambda \approx \lambda_{D_i} = \sqrt{T_i/4\pi e^2 n_i}$, provided the electron-to-ion temperature ratio $\tau = T_e/T_i$ is large.

The calculation of the ion drag force F_I involves the integration of the momentum-transfer cross section

over the ion velocity distribution (shifted Maxwellian distribution in our case) [3]. The major contribution to the momentum transfer comes from the region $v \sim v_{T_i}$ [the contribution from small velocities vanishes since the cross section has a weak (logarithmic) dependence on velocity; high velocities are not important due to the exponential factor in the velocity distribution]. Therefore, the characteristic value of β is given by $\beta(v_{T_i})$. To get a simple estimation of F_I we assume $\sigma_{\Sigma} \sim \pi\rho_*^2$, where $\rho_* \sim \lambda \ln\beta(v_{T_i})$. Then we obtain $F_I \sim \pi\rho_*^2(v_{T_i})n_i T_i u/v_{T_i}$ (the exact integration gives a prefactor of about 2). Hence, the ion drag force is proportional to $T_i^{3/2} m_i^{1/2}$ but depends only logarithmically on a , n_i , and τ .

Let us define the range of parameters where our estimation of the ion drag is valid. We take typical bulk plasma parameters: Ar gas, $T_i = 0.025$ eV, $\tau = 100$, $n_e = n_i = 10^9$ cm^{-3} . This gives $\beta(v_{T_i}) \approx 6a$ (where a is in μm) as long as $a < \lambda_D$, which is the usual situation in complex (dusty) plasmas. Then the inequality $\beta(v_{T_i}) > \beta_{\text{cr}} \approx 13.2$ can be easily satisfied for grains of a few microns. In this case, the results obtained for $\beta \ll 1$ [8] and $\beta \leq 5$ [3] are not applicable, but the expression derived in this Letter should be used instead. Our model also assumes “isolated” dust grain and “collisionless” ions. This means that the average interparticle distance and the ion mean free path both exceed the characteristic interaction length ($\sim \rho_*$). For the chosen parameters we have $\rho_*(\beta_{\text{cr}}) \approx 100$ μm , which gives the pressure range $p \lesssim 20$ Pa.

In conclusion, the scattering in the attractive screened Coulomb (Yukawa) potential was studied in the limit of strong interaction (interaction radius is larger than the screening length). We derived an analytical expression for the momentum-transfer cross section and applied it to estimate the ion drag force in complex (dusty) plasmas.

*Electronic address: skhrapak@mpe.mpg.de

- [1] L. D. Landau and E. M. Lifshitz, *Mechanics* (Pergamon, Oxford, 1960).
- [2] R. L. Liboff, *Phys. Fluids* **2**, 40 (1959).
- [3] S. A. Khrapak *et al.*, *Phys. Rev. E* **66**, 046414 (2002).
- [4] H.-S. Hahn, E. A. Mason, and F. J. Smith, *Phys. Fluids* **14**, 278 (1971).
- [5] M. D. Kilgore *et al.*, *J. Appl. Phys.* **73**, 7195 (1993).
- [6] J. E. Daugherty *et al.*, *J. Appl. Phys.* **72**, 3934 (1992).
- [7] S. A. Khrapak, A. V. Ivlev, and G. Morfill, *Phys. Rev. E* **64**, 046403 (2001).
- [8] M. S. Barnes *et al.*, *Phys. Rev. Lett.* **68**, 313 (1992).
- [9] G. E. Morfill *et al.*, *Phys. Rev. Lett.* **83**, 1598 (1999).
- [10] J. Goree *et al.*, *Phys. Rev. E* **59**, 7055 (1999).
- [11] S. Khrapak *et al.*, *Phys. Plasmas* **10**, 1 (2003).
- [12] U. Konopka *et al.*, *Phys. Rev. E* **61**, 1890 (2000).
- [13] D. Montgomery, G. Joyce, and R. Sugihara, *Plasma Phys.* **10**, 681 (1968).
- [14] G. Cooper, *Phys. Fluids* **12**, 2707 (1969).